Atomic structures and dynamic properties of dislocations in semiconductors: - Current progress and stagnation

Atomic structures and dynamic properties of dislocations in semiconductors: - Current progress and stagnation

Ichiro YONENAGA
Tohoku University, Sendai 980-8577, Japan
E-mail: *yonenaga@imr.tohoku.ac.jp*

Abstract

The current understanding of various dislocation phenomena, including nucleation, core structures, kink properties, impurity effects, and point defect formation and absorption in semiconductors, especially in terms on their dynamics, is comprehensively surveyed along with glide mechanism in wide-gap semiconductors. Even now, the experimental clarifications at an atomic scale for some dislocation phenomena are limited as being in Labyrinth in spite of the increasing knowledge addressed from developing computational simulations. In the stagnation, simultaneous in-situ and high-resolution imaging studies of dislocation phenomena are expected as an indispensable clue to further elucidate the dislocation phenomena.

1. Introduction

The increasing miniaturization and large-scale integration of modern semiconductor devices demand an accurate understanding of structural defects, such as dislocations, impurity-defect complexes, and so forth, which are essential entities in the device functions. These devices' atomic and electronic structure characterizations are the subject of intense experimental and theoretical investigations. Significant long-standing efforts using various microscopic imaging methods have succeeded in providing structural information regarding the defects in real space and have established them as dislocations emitted from a crack tip, misfit dislocations in epitaxy growth, etc. Such structural images have provided novel basic knowledge of today's exceedingly useful materials technology, and sometimes those images are artistic quality. However, owing to social demand and fickle interest in the latest materials, some defect-related phenomena still remain unclear/unresolved or are considered of little importance.

Figure 1 is a weak-beam transmission electron microscopic (WB-TEM) image of dislocations in deformed InP taken approximately 25 years ago. Dislocations marked "A" were generated at the left-side edge of the sample and travelled toward the inside, elongating the segments parallel to the surface during the observation at room temperature (RT). The dislocation motion may be assisted by electron-irradiated stimulation. It is possible that the dislocations did not reach a relaxed configuration. The top of the A dislocations was determined to be α-60° and glide-set, as seen from the tiny imaged stacking fault (SF). It should be noted that α dislocations moved but maintained a glide-set structure with a wide SF (~80 nm in a moment) during the observation at RT. Meanwhile, the "B" dislocation was dissociated widely, i.e., in glide-set, and accompanied an array of debris starting from point C. The dislocation was stable during the observation since those were induced by the deformation at 450°C. In this image we can identify several important dislocation and dislocation-related phenomena: nucleation, motion at RT (so-called low-temperature region), relevant core structure in motion, the formation of or interaction with point defects, etc. These are discussed in the quite long term and even now very exciting for us. However, whether these topics are well clarified or are being satisfactorily understood must be considered.

Many problems regarding the dislocation phenomena have been clarified by many researchers, but some unsolved topics still remain. In addition, owing to the significant development of experimental techniques and ab initio calculations, recent findings have made previously established consensuses controversial. For example, there are various discrepancies regarding several physical aspects of dislocation dynamics such as the brittle-to-ductile transition (BDT), shuffle- and glide-set dislocations, and atmospheric-confining pressure, even in Si. In this study, several microscopic aspects of dislocations and related phenomena in semiconductors noted above are comprehensively viewed along with impurity effects and dislocation mobilities in current wide-band-gap semiconductors. We primarily discuss what has been elucidated and, what has yet to be explored regarding the dislocation phenomena, which could stimulate the interest of researchers in this field in order to establish and develop our knowledge elementarily and

practically. Twenty years ago, Professor George reviewed the plasticity of semiconductors from a viewpoint similar to that of the present study [1]. The readers can refer his review to understand some of the advances made in this field.

2. Dislocation motion and core structures

2.1. Core structures of dislocations

The possible Burgers vector of a dislocation in the diamond cubic and sphalerite structure crystals is $\boldsymbol{b}=a/2<1\bar{1}0>$, moving on the {111} slip planes. Dislocations are energetically stable when they are parallel to the <110> directions on the slip planes in the crystals along the high Peierls potential valley. Such a dislocation can move on the plane situated between widely or closely spaced atomic planes, i.e., shuffle-set or glide-set, respectively, in Hirth and Lothe's model [2]. From a geometrical perspective, a dislocation on the glide-set plane is dissociated into two Shockley partial dislocations bounding a ribbon of intrinsic SF. The SF width, typically approximately 6–10 nm, is governed by the SF energy [3]. However, a dislocation in the shuffle-set plane is perfect since there are no stable SFs on the shuffle planes.

Duesbery and Joós re-examined the core structure of dislocations in motion in terms of line energy [4]. Their whistle addressed the long-term controversy regarding whether a dislocation controlling the plastic deformation of a semiconductor crystal is a glide-set or shuffle-set. Then, an extensive number of microscopic observations and theoretical discussions on dislocations and their structures in several semiconductors have been conducted through plastic deformation and related fractures under various conditions, such as under a confining pressure, with a micro- or nano-pillar and membrane specimen, and through indentation (including nano-method) [6-12].

2.2. Yield strength

Figure 2(a) shows the dependence of yield or fracture strength of Si crystals on temperature, from RT to 1300˚C [13]. As shown in the figure, the dependence is composed of two regions, extremely different features of which are distinguished at approximately 400˚C in Si crystals: one region is a plateau with no or extremely weak temperature dependence, and the other is a steep temperature-dependent region below and above the temperature. In the latter region, the yield strength τ_y in the elevated temperature region can be described as a function of temperature T and strain rate $\dot{\varepsilon}$ by the following empirical equation:

$$\tau_y=A\dot{\varepsilon}^{1/n}\exp(U/k_BT), \quad (1)$$

where A, n, and U are constants. n is reported to be ≈3, and k_B is the Boltzmann constant.

In researches regarding Si, there currently seems to be some consensus that dislocations are dissociated at temperatures higher than the BDT (hereafter referred to as a high-temperature region), and dislocations are considered perfect below the BDT (a

low-temperature region), i.e., at high stress and low temperature, based on TEM observations [9, 14-16]. In the intermediate-temperature region around BDT, there may be a transient deformation mode just as glide of mobile partial dislocations, leading to twins [5, 17, 18].

In some III-V compounds similar features are evident: Suzuki et al. reported a plateau of yield stress-temperature dependence of GaAs, GaP, InP, and InSb, all of which were deformed at the low temperature region under hydrostatic pressure [6]. Kedjar et al. [19] and Wheeler et al. [20, 21] also found similar features in GaAs and InSb in the compressive deformation of a pillar specimen, as shown in Fig. 3(a) [6, 19, 21, 22]. In addition, Kedjar et al. observed that shuffle-set dislocations in InSb deformed at temperatures below RT, as shown in Fig. 4 [23].

2.3. Dislocation velocity

It is also important to consider what we know about such dislocation structures in a viewpoint of their velocity. Figure 2(b) shows the velocities of an isolated 60˚ dislocation in high-purity Si in a temperature range from 350 to 1300˚C reported by various groups using a variety of experimental methods, including the in situ X-ray topographic and high-voltage TEM technique [13, 17, 24]. Here, it should be noted that the experimental results regarding such dislocation velocities were obtained only at temperatures above 300˚C. Overall, including our preliminary result from 400 to 700˚C, indicated by a red line, the temperature dependence of dislocation velocities reported by the groups falls into a narrow band with the same slope, except for the high-temperature region close to the melting temperature [13]. There seems no evidence of the temperature dependence of dislocation velocities explicitly different from that observed in the plasticity. Indeed, the dislocation velocity v is well expressed by the following empirical equation as a function of applied shear stress τ and temperature:

$$v=v_0(\tau/\tau_0)^m\exp(-Q/k_BT),\ \tau_0=1\ \text{MPa}, \quad (2)$$

where v_0, m, and Q are constants. The magnitudes of the stress exponent m and the glide activation energy Q reported by various groups are one or slightly higher than unity and 2.20–2.40 eV, respectively, though Q decreases to approximately 1.8 eV under high stress, especially at low temperatures. In microscopic structural studies, Alexander's group showed widely extended dislocations in a specimen moved in 325–422˚C under stress of 294 MPa [25, 26]. Conversely, we found that the dislocations investigated were shuffle-set at temperatures as high as 500˚C, though twin formation was observed in the temperature region between 400 and 550˚C, as previously reported by Yasutake et al. [17].

Figure 3(b) shows the velocities of α, β, and screw dislocations in InSb in a temperature from 50 to 300˚C reported by various groups [27-29]. The results currently available in literature show a similar feature to that observed in Si: the unique activation energies Q for respective dislocation types in a wide temperature range.

2.4. Elementary process of dislocation glides

In this review, the elementary process of dislocation glides in semiconductors consists of the thermally activated nucleation of a kink pair of critical separation on a dislocation line lying along the Peierls valley and the subsequent migration of the nucleated kink along the dislocation line as a second-type Peierls potential [2]. At present, it is commonly accepted that the velocity of a dislocation is described as follows [13]:

$$v=(bh^2\nu_D/k_BT)\tau L\exp[-(F_{kp}+W_m)/k_BT], \quad (3)$$

$$F_{kp}(\tau)=2F_k-f(\tau), \quad (4)$$

$$f(\tau)=\sqrt{(\mu\tau b^3h^3/2\pi)}, \quad (5)$$

where b is the magnitude of the Burgers vector $\boldsymbol{b}$ of a dislocation, h is the distance between adjacent Peierls valleys [$h=(\sqrt{3})b/2$], ν_D is the Debye frequency attempting kink formation and migration, L is the length of the moving dislocation, μ is the shear modulus, W_m is the migration energy of a kink, and F_{kp} is the formation energy of a kink pair determined by the formation energy of a single kink F_k. As known in Eq. (5), a kink pair formation is assisted by an applied stress. Though the dislocation velocity increases linearly with the length of the moving dislocation L in Eq. (3), currently, the velocity is considered to become length-independent at around 1–2 μm since the kink migration is considered to be impeded by some localized obstacles on the mean separation L^* along the dislocation line [30, 31], where L in Eq. (3) is replaced by L^*. If a dislocation is dissociated (glide-set), a partial dislocation glides according to the kink diffusion mechanism, as in the case of a perfect dislocation, where b in Eq. (3) should be replaced by b_p ($=b/\sqrt{3}$). Here, it should be noted that Eq. (3) corresponds to the so-called kink-collisionless case according to Hirth and Lothe's model. In a kink-collision case, wherein a kink collides and annihilates another kink of the opposite sign generated on the same line, Eq. (3) is changed to $v=(b^2h^2\nu_D/k_BT)\tau\exp[-(F_{kp}/2+W_m)/k_BT]$. Up to now, the kink-collision case has not been reported experimentally.

Eq. (3) has a form similar to the experimentally determined one of Eq. (2) with respect to the dependence of the dislocation velocity on stress and the temperature. The glide activation energy Q in Eq. (2) is the sum of F_{kp} and W_m in Eq. (2) as $Q=2F_k-f(\tau)+W_m$. Distinguished determinations of activation energies of F_k and W_m are limited in in situ stressing experiments using TEM or high-resolution (HR) TEM [14, 32, 33, 34], as shown in Table 1. The activation energies F_k and W_m for kinks on glide-set dislocations or partial dislocations sufficiently correspond to those derived computationally [35, 36] and also experimentally determined Q in consideration of the applied stress. The glide-set dislocations move in a correlated kink process on their paired partial dislocations. Computed activation energies of F_k and W_m for kinks on a shuffle-set dislocation are also shown in Table 1. It is remarkable that W_m is very small, though up to now, there have been no experimental reports on F_k and W_m for shuffle-set dislocations, except our preliminary result regarding dislocation velocities shown in Fig. 2(*b*).

2.5. Remaining uncertainties in shuffle-glide controversy

In the above shuffle-glide controversy described above, in terms of semiconductor plasticity, at present, we seem to have reached some consensus based on both experiments and theoretical evaluations, noted in section 2.2. Nevertheless, even now, there are some experimental findings in which partial dislocations can be observed in Si deformed at very high stress and at low temperature [9, 10]. Figures 5(*a*) to 5(*c*) shows HRTEM images of a shuffle-set 60˚, a glide-set 60˚, and a glide-set screw dislocation, respectively, observed in a GaAs specimen deformed at 450˚C. That is, shuffle- and glide-set dislocations coexist in the specimen. The condition is the so-called high temperature [37, 38].

Okuno and Saka reported that dislocation morphologies depended on the temperature scratched or indented in Si crystals. The observed shuffle-set dislocations were straight, triangular, zig-zag, and circular with increasing temperature, and the glide-set dislocations were circular [16]. In addition, such circular shuffle-set dislocations transited to glide-set ones by annealing at 300−350˚C. The transformation of dislocations from shuffle-set to glide-set is currently being modeled by several research groups [39-41].

The results of Okano-Saka noted above suggest an important point: Straight dislocations may be difficult to multiply themselves. This implies that such dislocations nucleated from the surface or sub-surface region and moved under stress. It is possible that, microscopically, the dislocation motion is rate-controlled by kink migration along the dislocation line if the kinks are also formed from the surface. Strangely, the stress–strain curves reported in deformation under a confining pressure were not accompanied by yielding or subtle yielding phenomena perhaps because the confining media damage specimen surfaces during the deformation. Thus, we can consider the plateau shown in Figs. 2(a) and 3(a) to be controlled by dislocation nucleation rather than kink motion.

3. Dislocation nucleation

In a crystal, a dislocation nucleates and then moves and multiplies. Therefore, nucleation is the initiation of various dislocation phenomena, which is an essential and long-standing issue of great interest among a variety of researchers in materials science. However, dislocation nucleation at an atomic level occurs in a single moment and only takes place once. Such dislocation nucleation is often unintentionally recognized as a result of nucleation and motion in some micro-scale distance in the crystal, as described in Fig. 1. From such postmortem images, the cause and the underlying microscopic and atomic mechanism are speculated.

Dislocations nucleate heterogeneously more easily at higher temperatures and under magnitude of stress that are much less than what is theoretically supposed, followed by means of their motion and multiplication. Such heterogeneous nucleation sites include surface irregularities, inner inclusions, and interfacial misfits with foreign matters. Surface irregularities include cracks, flaws, or steps induced by abrasion, scratching, or indentation. They are microscopic regions with strongly disturbed atomic structures that may be induced

by some energetic stimulation, such as a thermo-mechanical shock or a chemical reaction at the surface that is inevitably or accidentally involved in the crystal preparation process.

A large number of microscopic observations, including those by TEM, have been conducted on the nucleated dislocations in semiconductors, which has contributed to the establishment of wide knowledge in materials science and addressed the control and avoidance of dislocation nucleation in semiconductor technology. In Si, a tiny amorphous region is induced through a phase transformation by a concentration of an even subtle load during surface scratching or indentation at RT [42]. Such an amorphous region again becomes crystalline, accompanying a dislocated micro-region at elevated temperatures of approximately 500˚C. Conversely, dislocations nucleate from a load concentrated site without amorphization in some compound semiconductors with a high phase transformation pressure, such as GaAs [43]. Dislocation emission from a crack tip governs a phenomenon of fracture or plasticity, just like the BDT. Precipitates and inclusions also work as dislocation sources inside a crystal typically known through the punched-out mechanism. Misfit dislocations are generated by hetero-epitaxial growth and serve to relax strains originating in the lattice constant difference between the film and substrate, which is a key issue in widely adopted epitaxial technology.

Figures 6(*a*) and 6(*b*) show X-ray topographic images of dislocations detected in Czochralski (CZ)-grown crystals. This macroscopic method allows one to understand nucleation and the development of dislocation in one glance. Figure 6(*a*) shows dislocations inside a Dash necked part of a CZ-Si crystal to be <110> {111} slip systems. They were tentatively confirmed to generate and glide on {111} slip planes at approximately 1100˚C based on a cell structure locally constructed during the growth. Figure 6(*b*) shows dislocations generated from periphery facets developed in a diameter-increasing part of CZ-Si. Such facets act as preferential sites for twins. Dislocation generation phenomena during crystal growth are of significant interest but have yet to be explored in depth.

As noted above, though there have been many experimental and theoretical contributions to dislocation nucleation in semiconductors, nucleation itself still cannot be quantitatively clarified. At an atomic level, dislocation nucleation exceeds the bounds of dislocation theory. The most challenging experiment was an in-situ nano-indentation in a TEM by Minor et al. [15]. They directly observed dislocation plasticity in Si at RT and detected dislocation nucleation and metal-like plastic flow. Unfortunately, the time and spatial resolutions were so limited that the initial stage of dislocation nucleation could not be understood well.

Given this difficult situation, some groups are currently attempting to model dislocation nucleation through ab initio calculations at an atomic scale beyond the conventional flame of dislocation theory. Izumi's group derived that the activation energy of a shuffle-set dislocation for nucleation from a sharp corner in Si is lower than that of a glide-set one under stress of approximately 4 GPa [44]. Similarly, Pizzagalli's group revealed that, from a surface step of atomistic heights in Si, dislocations nucleate and propagate in the glide-set planes at high temperatures and low stresses and in the shuffle-set planes at low

temperatures and high stresses [45]. Recently, the group succeeded in mimicking formation of misfit dislocations and their networks in a GeSi-on-Si hetero-epitaxial system at an atomic scale [46].

4. Dislocation-point defect interaction

4.1. Dislocation activities affected by impurities

A dislocation interacts with impurities through the overlap of their strain fields or electrostatic fields. Generally, such interactions result in the reduction of the velocity of dislocations, and thus, the extra energy necessary to overcome the potential barrier related to the interaction is not consumed. A variety of impurities in semiconductor crystals affect the dynamic activities of individual dislocations through two kinds of microscopic mechanisms with respect to the stress range: one is the immobilization/release of dislocations, and the other is a modification of the dislocation mobility in glide motion. Regarding energy, the former is related to agglomeration and the cluster/complex formation of certain kinds of impurities, known as "gettering," where dislocations are in rest by them or move in slow motion overcoming mainly their strain field [47-51]. The latter pertains to the electrostatic effects of individually dispersed impurities within the crystal.

Dislocation velocities depend on impurity species and their concentration [47]. Figure 7 shows how the dislocation velocities in Si vary depending on the concentration of impurities in a semi-quantitative manner. The dislocation velocities are those at 700˚C under a stress of 30 MPa, where the measured velocities are thought to be free from the influence of impurity immobilization. The dislocation velocities in Si doped with donor impurities (P, As, and Sb) increases remarkably (as does the dislocation velocity in Si doped with acceptor impurity B) from that in high-purity Si as the concentration of these impurities increases. Neural impurities have almost no effect on the enhancement/retardation of dislocation velocity.

Figure 8 shows the velocities of dislocations in Si doped with various impurities plotted against the reciprocal temperatures. The velocity of the dislocations in motion is not affected by the doping of Si crystals with neutral impurities in the investigated temperature range. The dislocation velocities are significantly larger in P- and As-doped Si and slightly larger in B-doped than those in high-purity Si at temperatures lower than approximately 800˚C, where the concentration of electrically active impurities is higher than the concentration of the intrinsic carrier. The velocities are described by Eq. (1) as a function of stress and temperature. The velocity enhancement and weak temperature dependence in n-type crystals, i.e., reduction of the glide activation energy Q, are attributed to the electronic effect through the formation and/or migration of kinks on a dislocation as an elementary process of dislocation motion. An acceptor level is associated with a kink site in Si, as proposed by Hirsch [52] and Jones [53]. Similarly, a donor level may be associated with a kink site in B-doped Si. Since the reduced amount of Q in the crystals in comparison with that of high-purity Si depends on the Fermi level of the crystals, it can be supposed that a dislocation has a kink with an acceptor level and a donor level in the band gap at ~0.5 and

~0.25 eV, respectively, above the valence band edge E_v. Indeed, the result corresponds well to the theoretical estimation of E_v+0.55 and 0.34 eV, respectively, estimated by Heggie and Jones [54].

In Ge, a dislocation is known to accompany an acceptor level in the band gap at ~0.15 eV above the E_v [55, 56]. It is possible that there is a donor level inside the valence band. If a kink in a stable configuration accompanies such an acceptor (donor) level, the equilibrium concentration of the kinks on the dislocation may increase in an n-type (p-type) crystal since the free energy of the system decreases if such acceptors (donors) accept electrons from chemically given donors (acceptors). However, if an acceptor (donor) level is associated with a kink in the saddle point configuration of motion, the migration energy of a kink may be reduced and lead to a higher mobility of the kink. In both cases, the velocity of the dislocation is enhanced. Currently, in macroscopic studies that evaluate dislocation velocities, it is difficult to verify the above details since there is no information regarding kink formation or migration energies along a dislocation. Direct atomistic characteristics of core structures and kinks of dislocations in electronic states are indispensable for comprehensive understanding of the mechanism.

It should be noted that, even at temperatures higher than 800˚C, the dislocation velocity in Si doped with B, P, and As impurities is larger than that in high-purity Si. Instead of the above-mentioned electronic mechanism, the kink configuration may be modified in the elementary process of dislocation motion in heavily impurity-doped semiconductors, where the doping level is extremely high and thus regarded as a rather dilute solid solution.

The electrical effects on the enhancement and retardation of dislocation motion become complicated in Ill-V compound semiconductors [21, 50, 57]. Figures 9(*a*) and 9(*b*) show how the velocities of α, β, and screw dislocations in GaAs and InP depend on the electrical properties of impurities in a semi-quantitative manner. In GaAs, the velocities of β and screw dislocations are enhanced by the doping of acceptor impurities and retarded by the doping of donor impurities. Meanwhile, the velocity of α dislocations is retarded by the doping of both acceptor and donor impurities. In the model adopted in Si, 30˚ β-type Shockley partials in GaAs may accompany kinks associated with donor levels located in the upper part of the band gap. Conversely, 90˚ α-type Shockley partials in InP may have kinks associated with acceptor levels located in the lower part of the band gap. As shown here, striking is the fact that the effect varies depending on material and also on impurity species. Currently, the situation in compound semiconductors is ambiguous certainly because of the lack of experimental evaluations of dislocation velocities and theoretical studies regarding the materials and partly because of the fact that materials available for such researches are limited and almost impossible to find.

4.2. Dislocation motion related to point defect accumulation and formation

As shown in Fig. 1, dislocations generate some point-like defects (so-called debris) that trail from specific sites, called a jog. It is known that the plastic deformation of semiconductors is associated with the formation of non-equilibrium intrinsic point defects

(vacancies or interstitials) that can be left in the trace of a dislocation's glide plane, resulting in the formation of loops or small complexes. Characteristically, in semiconductors, these defects possess electrical, optical, and magnetic properties, resulting in some confusion because their signals and data appear to overlap with those of intrinsic dislocations.

Figure 10 illustrates typical trail defects in Si observed by an electron-beam-induced current (EBIC) image reported by a Russian group [58]. The dark contrasts are based on the motion of dislocations generated from the scratch during stressing at 600˚C. Since 1981, when these trail defects were first detected, the Russian group has conducted several studies, mainly using EBICs [59, 60]. Recently, Kveder et al. reported that most of these trail defects are electrically inactive complexes of a vacancy and an unknown defect [61]. In the figure, however, it is unclear why the image develops only on the one side of the scratch since dislocations swept on both sides. Some differences might exist in the core structure of glide-set dislocations moved upward and downward from the scratch. Studies at a microscopic or atomistic scale are significantly limited because of their low densities and point-like sizes. Point defects dominant in thermal equilibrium at temperatures are thought to be vacancies rather than self-interstitials. Recently, Fedina et al. reported clustering of vacancy and interstitial pairs for so-called {113}-defect formations during in-situ HREM irradiation [62]. They found planar fourfold-coordinated defects in the process, though it remains unclear whether such kinds of point-like defects are detectable using that method. For accurate understanding, the thermodynamics of such point defects should be considered, and their formation and migration energies should be included.

Dislocations may absorb generated point defects, resulting in a climb. A climb of dislocations is a fundamental process in addition to their glide and plays an essential role in their recovery. Climbed screw dislocations in well-developed helix shapes were found in the emitter region of a Si bipolar transistor [63]. Up until now, a limited number of qualitative studies have been conducted at a microscopic and/or atomistic scale. According to conventional knowledge, a dissociated dislocation should constrict in advance when it undergoes climb, forming a jog, since an SF is not supposed to climb by absorbing point defects. However, climb phenomena in irradiated or quenched semiconductors are somewhat different. In electron-irradiated Si and GaAs, dissociated dislocations were confirmed to undergo climb without the constriction of SF or being tangled with prismatic dislocations after the climb [64-66]. Thus, it was thought that the climb of an extended dislocation was first facilitated by the condensation of point defects into prismatic dislocation loops along both partials to form extended jogs on the dislocation. Indeed, the climb of a partial dislocation absorbing interstitials in GaAs was observed by HREM [67].

Figure 11 shows a weak beam image of a dislocation that has undergone climb by absorbing interstitials emitted during oxygen precipitation in Si annealed at 900˚C for 48 h [68]. The dislocation is dissociated over the entire observed length with a distance of approximately 10 nm from the original position given by the array of precipitates. Interestingly, the dislocations remained fully dissociated without visible constrictions or small prismatic loops. Under a low supersaturation or slow supply of point defects, the climb of

dissociated dislocations may proceed according to the model of Thomson and Balluffi [69]. Quantitative and kinematic clarification of the climb should be conducted through a series of suitable experimental set-ups to evaluate osmotic force due to excess point defects.

5. Dislocation motion in wide band-gap semiconductors

Currently, some compound semiconductors with band gap wider than approximately 3 eV have attracted keen interest as applications to blue- and ultraviolet-light-emitting devices, high power switching devices, photo-detectors, and chemically stable substrates. Knowledge of dislocation characteristics and dynamic properties is essential in such semiconductors both as a physical basis and for controlling dislocation generation and deformation during crystal growth and device processing. Indeed, some studies using micro pillar samples have been conducted, primarily around RT [70, 71]. However, knowledge of such semiconductors is significantly limited compared with that in semiconductors with diamond and sphalerite cubic structures (except SiC) [18]. The reason for this may partially be due to the low crystallographic symmetry of the wurtzite (hexagonal) structure, low crystallinity, or the limited size available for dynamical characterizations. Here, we briefly review our results regarding the mechanical strength of typical wide-band-gap semiconductor crystals obtained through a conventional compressive deformation at elevated temperatures in order to derive the characteristic properties of dislocation mechanisms common in semiconductors.

Figure 12 shows the yield stresses of various wide-band-gap crystals plotted against reciprocal temperature along with that of Si [72-74]. The yield stresses of GaN, AlN, and SiC are approximately 100–200 MPa, even at 1000˚C, and those of ZnO are approximately 15 MPa at 650˚C, while is lower than those of GaN and SiC. As shown in the figure, the yield stress of SiC is higher in slip along the prismatic m-$\{1\bar{1}00\}$ plane than along the basal c-(0001) plane [73]. In addition, GaN shows yield stress dependence on the slip plane, higher in the order of pyramidal p-$\{11\bar{2}2\}$, m-$\{1\bar{1}00\}$, and c-(0001) one, and ZnO shows slightly weak dependence. Future researchers should strive to confirm the operated pyramidal slip plane microscopically.

It was found that the yield strength of the wide-band-gap semiconductors of the wurtzite structure showed clear dependence on reciprocal temperature, same as that of the diamond and sphalerite semiconductors, expressed as a function of temperature and strain rate by Eq. (1). In the established concept of the dislocation dynamics of deformation, the macroscopic plasticity of various semiconductor crystals is rate-controlled by the collective motion of individual dislocations [21, 75]. Thus, the yield strength of Eq. (1) relates to the dislocation velocity of Eq. (2), where the characterizing parameters n, U, m, and Q in the equations are related as follows:

$$m=n-2,\ Q=U*n. \tag{6}$$

If the relations also remain valid in wide-band-gap semiconductors with the wurtzite structure,

the magnitudes of the glide activation energy Q of dislocation motion can be estimated, for example, as 2–2.7 and 0.7–1.2 eV in GaN and ZnO, respectively. Dislocations in ZnO are mobile, as has generally been assumed. Weingarten and Chung derived Q=1.6 eV for a (a/3) $[11\bar{2}0]$-type dislocation gliding on the c and m planes of GaN from molecular dynamics simulations [76]. Plausible reasons for the difference of Q obtained by the experiment and calculation in GaN may be due to the simplified model used to track the motion of a single dislocation in the calculation. More detailed experiments would likely be fruitful.

Though the velocity and glide activation energy Q for dislocation motion vary from semiconductor to semiconductor, Q is known in phenomenology to increase linearly with the band-gap energy in various semiconductors in each group of the elemental and IV–IV compound, III–V compound, and II–IV compound semiconductors irrespective of differences in the diamond, sphalerite, or wurtzite structure. In the above phenomenological dependences, the gradient of the line varies in the order of elemental, III–V, and II–VI compounds, which is possibly related to the ionicity of the semiconductors [77]. Figure 13 shows the glide activation energies of dislocation motion Q, experimentally determined in wide-band-gap semiconductors, plotted as a function of Gb^3, that is, the energy of a minimum-length b of dislocation [30]. As shown in the figure, there is a linear correlation between Q and Gb^3 in semiconductors. G reflects the atomic bonding character that involves the iconicity, and b is the magnitude of the Burgers vector of dislocation, which is linearly dependent on atomic distance. This feature suggests that atomic bonding primarily controls the motion of dislocations. This supposition is also supported by the fact that various semiconductors show the hardness homology scaled by Gb^3 and G [78, 79].

It is important to correlate the phenomenological findings with microscopic dislocation mechanisms and energies for kink formation and migration (F_k and W) on a partial or perfect dislocation. Since the glide activation energies Q of the crystals are primarily determined by macroscopic plasticity studies, it is not sufficient to merely discuss the above subject. Unfortunately, this is the extent of our current knowledge. Future atomistic observations and evaluations in various types of semiconductors are inevitable.

6. Conclusive remarks to the microscopic-imaging community in future

This survey comprehensively reviewed the present understanding of the dynamic properties and atomic structures of dislocations in semiconductors for clarifying what information has been successfully elucidated and what remains unresolved. Though somewhat old images were adopted consciously, what does the reader think? Many subjects just as nucleation, core structure, kink properties of dislocations in motion, impurity effects, interactions with point defects, and glide mechanism, including wide band-gap semiconductors, remain unclear even at present. The situation is as “we are being confined in the Labyrinth.”

Central problems include the “atomic structure of dislocations” and their clarification is difficult without the assistance of theoretical studies. Indeed, recent

computational studies intensively conducted by the groups of Pizzagalli and Bulatov are making ahead. Such models should also be verified by detrimental imaging studies in order to develop understanding of the dislocation phenomena. Imaging studies of the dislocation structures at an atomic scale as a phenomenology require high spatial and fine time resolution. Though it is not easy to simultaneously realized these resolutions, in situ and high-resolution imaging studies, not postmortem ones, are expected to promptly impel the elucidation of the above noted topics in the consideration of stimulation by electron irradiation [30]. Indeed, an extraordinary plasticity of ZnS in darkness has recently been reported [80].

From a vast number of papers regarding dislocations in semiconductors, only a limited number of papers were introduced and/or cited in this short review. This is biased by the author's interest, for which the author is solely responsible.

Acknowledgment

The author expresses his gratitude to his colleagues Profs. Y. Ohno, T. Taishi, K. Kutsukake, Drs. Y. Tokumoto, and M. Deura for close and long-standing collaborations on dislocation researches. This chapter is dedicated to the memory of Professor Malcolm I. Heggie.

References

[1] George A 1997 Plastic deformation of semiconductors: some recent advances and persistent challenges *Mater. Sci. Tech.* **233** 88-102

[2] Hirth J P, Lothe J 1982 *Theory of Dislocations*, 2nd ed. (New York, Wiley)

[3] Gottschalk H, Patzer G and Alexander H 1978 Stacking fault energy and iconicity of cubic III-V compounds *Phys. Stat. Solidi* A **45** 207-217

[4] Duesbery M S and Joós B 1996 Dislocation motion in silicon: the shuffle-glide controversy *Philos. Mag. Lett.* **74** 253-258

[5] Castaing J, Veyssière P, Kubin L P and Rabier J 1981 The plastic deformation of silicon between 300˚C and 600˚C *Philos. Mag.* A **44** 1407-1413

[6] Suzuki T, Yasutomi T, Tokuoka T and Yonenaga I 1999 Plasticity of III-V compounds at low temperatures *Phys. Stat. Solidi* A **171** 47-52

[7] Nakao S, Ando T, Shikida M and Sato K 2008 Effect of temperature on fracture toughness in a single-crystal-silicon film and transition in its fracture mode *J. Micromech. Microeng.* **18** 015026

[8] Gerberich W W, Michler J, Mook W M, Ghisleni R, Östlund F, Stauffer D D and Ballarini R 2009 Scale effects for strength, ductility, and toughness in "brittle" materials *J. Mater. Res.* **24** 898-906

[9] Rabier J, Pizzagalli L and Demenet J L 2010 Dislocations in silicon at high stress *Dislocations in Solids* Vol. 16 (Hirth J P and Kubin L, ed.) (Amsterdam, Elsevier) p. 47-108

[10] Korte S, Barnard J S, Stearn R J and Clegg W J 2011 Deformation of silicon – Insights from microcompression testing at 25–500˚C *Int. J. Plast.* **27** 1853-1866

[11] Lauener C M, Petho L, Chen M, Xiao Y, Michler J and Wheeler J M 2018 Fracture of Silicon: Influence of rate, positioning accuracy, FIB machining, and elevated temperatures on toughness measured by pillar indentation splitting *Mater. Design* **142** 340–349

[12] Merabet A, Texier M, Tromas C, Brochard S, Pizzagalli L, Thilly L, Rabier J, Talneau A, Le Vaillant Y -M, Thomas O and Godet J 2018 Low-temperature intrinsic plasticity in silicon at small scales *Acta Mater.* **161** 54-60

[13] Yonenaga I 2015 An overview of plasticity of Si crystals governed by dislocation motion *Eng. Fract. Mech.* **147** 468-479

[14] Kolar H R, Spence J C H and Alexander H 1996 Observation of moving dislocation kinks and unpinning *Phys. Rev. Lett.* **77** 4031-4034

[15] Minor A M, Lilleodden E T, Jin M, Stach E A, Chrzan D C and Morris Jr J W 2005 Room temperature dislocation plasticity in silicon *Philos. Mag.* **85** 323-330

[16] Okuno T and Saka H 2013 Electron microscope study of dislocations introduced by deformation in a Si between 77 and 873 K *J. Mater. Sci.* **48** 115-124

[17] Yasutake K, Shimizu S, Umeno M and Kawabe H 1987 Velocity of twinning partial dislocations in silicon *J. Appl. Phys.* **61** 940-946

[18] Pirouz P, Samant A V, Hong M H, Moulin A and Kubin L P 1999 On temperature dependence of deformation mechanism and the brittle-ductile transition in semiconductors *J. Mater. Res*. **14** 2783-2793

[19] Kedjar B, Thilly L, Demenet J L and Rabier 2010 Plasticity of indium antimonide between −176 and 400˚C under hydrostatic pressure. Part I: Macroscopic aspects of the deformation *Acta Mater.* 58 1418-1425

[20] Chen M, Wehrs J, Michler J and Wheeler J M 2016 High-temperature in situ deformation of GaAs micro-pillars: Lithography versus FIB machining *J Metals* **68** 2761-2767

[21] Yonenaga I 1997 Mechanical properties and dislocation dynamics in III-V compounds *J. Phys. III France* **7** 1435-1450

[22] Wheeler J M, Thilly L, Morel A, Taylor A A, Montagne A, Ghisleni R and Michler J 2016 The plasticity of indium antimonide: Insights from variable temperature, strain rate jump micro-compression testing *Acta Mater.* **106** 283-286

[23] Kedjar B, Thilly L, Demenet J L and Rabier 2010 Plasticity of indium antimonide between −176 and 400˚C under hydrostatic pressure. Part II: Microscopic aspects of the deformation *Acta Mater.* **58** 1426-1440

[24] Yonenaga I, Imoto Y, Ohno Y, Kutsukake K and Deura M *Unpublished work*

[25] Wessel K and Alexander H 1977 On the mobility of partial dislocations in silicon *Philos. Mag.* **35** 1523-1536

[26] Küsters K H and Alexander H 1983 Photoplastic effect in silicon *Physica* B **116** 594-599

[27] Mihara M and Ninomiya T 1978 Dislocation velocities in III-V compound semiconductors *Oyo Butsuri* **47** 847-852 (in Japanese)

[28] Ossipyan Yu A and Shikhsaidov M Sh 1990 On the influence of carriers on the mobility of dislocations in semiconductors *Proc. Conf. on Defect Control in Semiconductors* (Sumino K, ed.) (Elsevier, Amsterdam) p. 1387-1391

[29] Kisel V P, Erofeeva S A and Shikhsaidov M Sh 1993 Dynamics of dislocations in InSb and GaAs crystals *Philos. Mag.* A **67** 343-360

[30] Maeda K and Takeuchi S 1996 Enhancement of dislocation mobility in semiconducting crystals by electronic excitation *Dislocations in Solids* Vol. 10 (Nabarro F R N and Duesbery M S, ed.) (Elsevier, Amsterdam) p. 443-504

[31] Vanderschaeve G, Levade C and Caillard D 2000 Transmission electron microscopy in situ investigation of dislocation mobility in semiconductors *J. Phys.: Condens. Matter* **12** 10093-10103

[32] Nikitenko V I, Farber B Ya and Lunin Yu L 1987 Experimental investigation of the dynamics of kinks of dislocation lines in semiconductor single crystals *Sov. Phys. JET*P **66** 738-746

[33] Louchet F, Pelissier J, Caillard D, Peyrade J P, Levade C and Vanderschaeve G 1993 In situ TEM study of dislocation mobility in semiconducting materials *Microsc. Microanal. Microstruct.* **4** 199-200

[34] Maeda K, Inoue M, Suzuki K, Amasuga H, Nakamura M and Kanematsu E 1997 High resolution electron microscopic studies of the atomistic glide processes in semiconductors *J. Phys. III France* **7** 1451-1467

[35] Cai W, Bulatov V V, Justo J F, Argon A S and Yip S 2000 Intrinsic mobility of a dissociated dislocation in silicon *Phys. Rev. Lett.* **84** 3346-3349
[36] Pizzagalli L and Beauchamp P 2008 Dislocation motion in silicon: the shuffle-glide controversy revisited *Philos. Mag. Lett.* **88** 421-427
[37] Yonenaga I, Lim S –H, Lee C -W and Shindo D 2001 Atomic arrangement of dislocation defects in GaAs by HREM *Mater. Sci. Eng.* A **309-310** 125-128
[38] Yonenaga I 2004 Atomic structure of defects in semiconductors *Encyclopedia of Nanoscience and Nanotechnology* Vol. 1 (Nalwa H S, ed.) (American Scientific Publishers) p. 135-145
[39] Rabier J 2013 On the core structure of dislocations and the mechanical properties of silicon *Philos. Mag.* **93** 162-173
[40] Li Z and R. C. Picu R C 2013 Shuffle-glide dislocation transformation in Si *J. Appl. Phys.* **113**, 083519
[41] Rodney D, Ventelon L, Clouet E, Pizzagalli L and Willaime F 2017 Ab initio modeling of dislocation core properties in metals and semiconductors *Acta Mater.* **124** 633-659
[42] Minowa K and Sumino K 1992 Stress-induced amorphization of a silicon crystal by mechanical scratching *Phys. Rev. Lett.* **69** 320-322
[43] Minowa K and Sumino K *Private communication*
[44] Shima K, Izumi S and Sakai S 2010 Reaction pathway analysis for dislocation nucleation from a sharp corner in silicon: Glide set versus shuffle set *J. Appl. Phys.* **108** 063504
[45] Godet J, Hirel P, Brochard S and Pizzagalli L 2009 Evidence of two plastic regimes controlled by dislocation nucleation in silicon nanostructures *J. Appl. Phys.* **105** 026104
[46] Maras E, Pizzagallil L, Ala-Nissila1 T and Jónsson H 2017 Atomic scale formation mechanism of edge dislocation relieving lattice strain in a GeSi overlayer on Si(001) *Sci. Rep.* **7** 11966
[47] Yonenaga I 2005 Dislocation–impurity interaction in Si *Mater. Sci. Eng.* B **124-125** 293-296
[48] Heggie M I, Jones R and Umerski A 1993 Ab initio total energy calculations of impurity pinning in silicon *Phys. Stat. Solidi* A **138** 383-387
[49] Yonenaga I and Sumino K 1996 Influence of oxygen precipitation along dislocations on the strength of silicon crystals *J. Appl. Phys.* **80** 734-738
[50] Yonenaga I and Sumino K 1989 Impurity effects on generation, velocity, and immobilization of dislocations in GaAs *J.Appl. Phys.* **65** 85-92
[51] Yonenaga I and Sumino K 1992 Behaviour of dislocations in GaAs revealed by etch pit technique and X-ray topography *J. Cryst. Growth* **126** 19—29
[52] Hirsch P B 1979 A mechanism for the effect of doping on dislocation mobility *J. Phys. Colloq. (Paris)* **40** C6-117-121
[53] Jones R 1980 The structure of kinks on the 90˚ partial in silicon and a 'strained-bonded model' for dislocation motion *Philos. Mag.* B **42** 213-219
[54] Heggie M I and Jones R 1983 Solitons and the electrical and mobility properties of dislocations in silicon *Philos. Mag.* B **48** 365-377

[55] Mura Y, Taishi T, Tokumoto Y, Ohno Y and Yonenaga I 2011 Impurity effects on the generation and velocity of dislocations in Ge *J.Appl. Phys.* **109** 113502
[56] Mura Y, Kutsukake K, Ohno Y, Tokumoto Y and Yonenaga I *Unpublished work*
[57] Yonenaga I and Sumino K 1993 Effects of dopants on dynamic behavior of dislocations and mechanical strength in InP *J.Appl. Phys.* **74** 917-924
[58] Bondarenko I E, Blumtritt H, Heydenreich J, Kazmiruk V V and Yakimov E B 1986 Recombination properties of dislocation slip planes *Phys. Stat. Solidi* A **95** 173-177
[59] Orlov V I, Yakimov E B and Yarykin N 2016 Spatial distribution of the dislocation trails in silicon *Solid State Phenom.* **42** 155-159
[60] Khorosheva M A, Kveder V V and Seibt M 2015 On the nature of defects produced by motion of dislocations in silicon *Phys. Stat. Solidi* A **212** 1695-1703
[61] Kveder V V, Khorosheva M A and Seibt M 2018 Concerning vacancy defects generated by moving dislocations in Si *Mater. Today: Proc.* **5** 14757–14764
[62] Fedina L I, Song S -A, Chuvilin A L, Gutakovskii A K and Latyshe A V 2013 The Mechanism of {113} Defect Formation in Silicon: Clustering of interstitial–vacancy pairs studied by in situ high-resolution electron microscope irradiation *Microsc. Microanal.* **19** S5 38–42
[63] Strunk H, Gösele U and Kolbesen B O 1979 Interstitial supersaturation near phosphorus-diffused emitter zones in silicon *Appl. Phys. Lett.* **34** 530-532
[64] Ourmazd A, Cherns D and Hirsch P B 1981 The climb of dissociated dislocations in semiconductors *Inst. Phys. Conf. Ser.* **60** 39-44
[65] Cherns D and Feuillet G 1985 The mechanism of dislocation climb in GaAs under electron irradiation *Philos. Mag.* A **51** 661-674
[66] Thibault-Desseaux J, Kirchner H K O and Putaux J L 1989 Climb of dissociated dislocations in silicon *Philos. Mag.* A **60** 385-400.
[67] Yonenaga I, Brown P D, Burges W G and Humphreys C J 1995 Faulted dipoles in In-doped GaAs *Inst. Phys. Conf. Ser.* **146** 87-90
[68] Minowa K, Yonenaga I and Sumino K 1991 Climb of extended dislocations in silicon caused by oxygen precipitation *Mater. Lett.* **1** 164-170
[69] Thomson R M and Balluffi R W 1962 Kinetic theory of dislocation climb. II Steady state edge dislocation climb *J. Appl. Phys.* **33** 803-812
[70] Wheeler J M, Niederberger C, Tessarek C, Christiansen S and Michler J 2013 Extraction of plasticity parameters of GaN with high temperature, in situ micro-compression *Intl. J. Plasticity* **40** 140–151
[71] Wheeler J M, Raghavan R, Wehrs J, Zhang Y -C, Erni R and Michler J 2016 Approaching the Limits of Strength: Measuring the Uniaxial Compressive Strength of Diamond at Small Scales *Nano Lett.* **16** 812-816
[72] Fujita S, Maeda K and Hyodo S 1987 Dislocation glide motion in 6H SiC single crystals subjected to high-temperature deformation *Philos. Mag.* A **55** 203-215
[73] Yonenaga I and Motoki K 2001 Yield strength and dislocation mobility in plastically deformed bulk single-crystal GaN *J. Appl. Phys.* **90** 6539-6541

[74] Yonenaga I, Koizumi H, Ohno Y and Taishi T 2008 High-temperature strength and dislocation mobility in the wide band-gap ZnO: Comparison with various semiconductors *J. Appl. Phys.* **103** 093502

[75] Yonenaga I and Sumino K 1992 Mechanical properties and dislocation dynamics of III-V compound semiconductors *Phys. Stat. Solidi* A **131**, 663-670

[76] Weingarten N S and Chung P W 2013 a-Type edge dislocation mobility in wurtzite GaN using molecular dynamics *Scripta Mater.* **69** 311-314

[77] Yonenaga I 1998 Dynamic behavior of dislocations in InAs: In comparison with III–V compounds and other semiconductors *J. Appl. Phys.* **84** 4209-4213

[78] Yonenaga I and Suzuki T 2002 Indentation hardnesses of semiconductors and a scaling *Philos. Mag. Lett.* **82** 535-542

[79] Yonenaga I, Deura M, Tokumoto Y. Kutsukake K and Ohno Y 2018 Insight into physical processes controlling the mechanical properties of the wurtzite group-III nitride family *J. Cryst. Growth* **500** 23-27

[80] Oshima Y, Nakamura A and Matsunaga K 2018 Extraordinary plasticity of an inorganic semiconductor in darkness: *Science* **360**, 772-774

Table 1. Magnitudes of F_k and W_m for dislocations in Si evaluated experimentally and theoretically [14, 32, 33, 35, 36].

Groups	*Dislocation type*	F_k (eV)	W_m (eV)
Experiments			
Nikitenko et al. (1987) [32]	Glide-set 60˚	0.5	1.6
Louchet et al. (1993) [33]	Glide-set 60˚	0.9	1.3
Kolar et al. (1996) [14]	Glide-set 90˚	0.73	1.24
Calculations			
Cai et al. (2000) [35]	Glide-set screw 30˚-30˚	0.7	1.2
Pizzagalli-Beauchamp (2008) [36]	Glide-set 30˚	0.8	1.24
Pizzagalli-Beauchamp (2008) [36]	Shuffle-set screw	1.13	0.09

Figure captions

Figure 1. WB-TEM image of dislocations in deformed InP. Dislocations A, 60˚ α glide-set, generated at the left-side edge and travelled toward the inside of the specimen. Dislocations B, widely dissociated (glide-set) accompanied an array of debris originating in point defects, starting from the point C.

Figure 2. (*a*) Yield strength of Si as a function of temperature [13]. (*b*) Velocities of 60˚ dislocations as a function of temperature. Marks and numerals in the figure can refer those in Ref. 13. The red dashed line shows velocities under a stress of 100 MPa [24]. Velocity of twins under 280 MPa is superimposed by a green dotted line [17]. The arrows show supposed core structures of dislocations. Marks and numerals in the figures can refer those in Ref. 13. (Modified under permission of Elsevier)

Figure 3. (*a*) Yield strength of InSb as a function of temperature, based on results of various authors [6, 19, 21, 22]. HP, pillar, and At means deformation condition under high confining pressure, of pillar specimen, and under atmosphere, respectively. (*b*) Velocities of α, β, and screw dislocations as a function of temperature in InSb reported by various groups [27-29].

Figure 4. Morphologies of dislocations dependent on the compressive-deformation temperature in InSb [23]. (Modified under permission of the authors and Elsevier.)

Figure 5. HRTEM images of (*a*) 60˚ shuffle-set, (*b*) 60˚ glide-set, and (*c*) screw glide-set dislocation observed in a GaAs specimen deformed at 450˚C [37, 38]. (Under permission of Elsevier)

Figure 6. X-ray topographic images of dislocations observed in (*a*) a neck and (*b*) periphery facets developed in a size increasing part of CZ-Si.

Figure 7. Velocities of 60˚ dislocations under a shear stress of 30 MPa at 700˚C in impurity-doped CZ–Si. Their dependence on the electrical type and concentration of main impurities. The ellipse marked GeB shows the result for Ge and B co-doped CZ–Si at concentrations of 4×10^{19} and 9×10^{18} cm^{-3}, respectively.

Figure 8. Velocities of 60˚ dislocations under a shear stress of 30 MPa in high purity Si and impurity-doped CZ–Si plotted against the reciprocal temperature. Numerals show the impurity concentration in a unit of cm^{-3}. GeB shows the results for Ge and B co-doped CZ–Si at concentrations of 4×10^{19} and 9×10^{18} cm^{-3}, respectively.

Figure 9. Impurity effects on the velocities of various types of dislocations under a shear stress of 20 MPa at 450˚C in (*a*) GaAs and (*b*) InP.

Figure 10. EBIC and etch pit images of dislocations started from the scratch at 600˚C in Si [58]. The area of the etch pit image is marked by the dotted line in EBIC image. (Modified under permission of the authors and Wily VCH)

Figure 11. WB-TEM image of a dislocation in CZ-Si underwent climbing during annealing at 900˚C for 48 h and illustration of the configuration [68]. (Modified under permission of Elsevier)

Figure 12. Yield stresses ty of the hcp-based crystals of AlN, GaN, ZnO, and 6H-SiC plotted against reciprocal temperature for deformation under a strain rate of $\sim 2\times10^{-4}$ s^{-1} in comparison with those of Si. “c”, “m”, and “p” show the results of deformation along the basal c-(0001), prism m-$\{1\bar{1}00\}$, and prism p-$\{11\bar{2}2\}$ planes, respectively. Some original data of SiC, GaN, and ZnO can be found in [72-74].

Figure 13. Activation energies of dislocation glide Q experimentally determined in wide band-gap semiconductors plotted as a function of Gb^3.

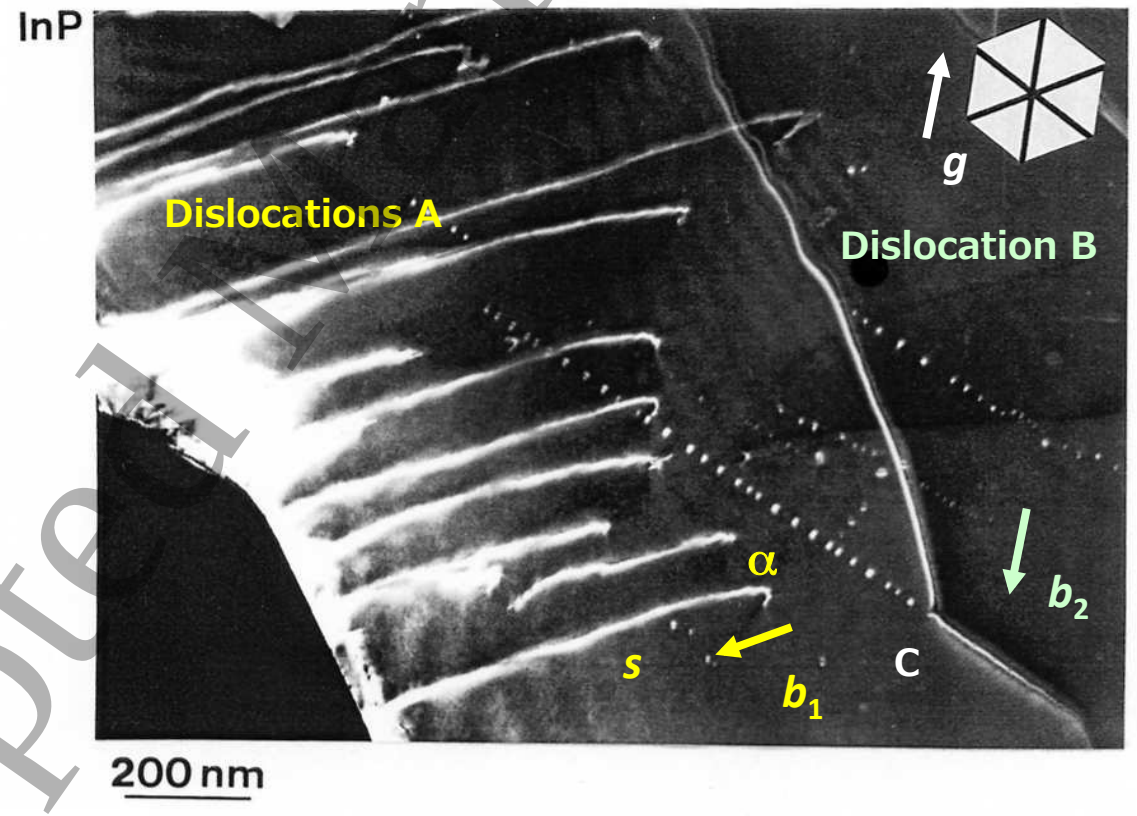

Fig. 1

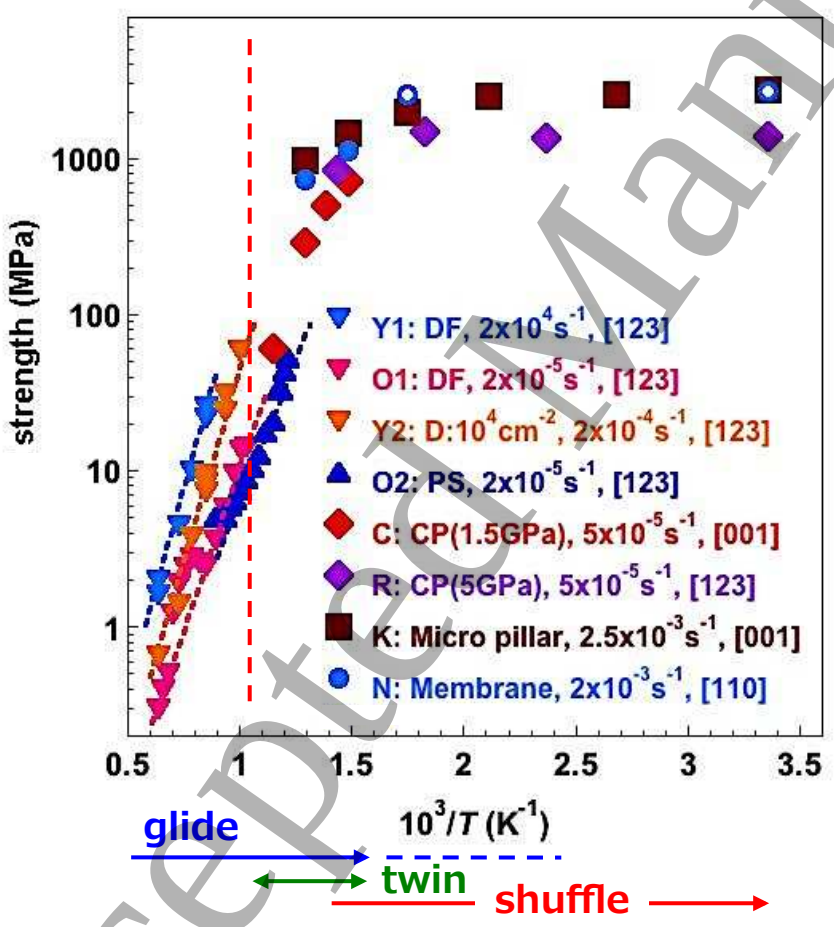

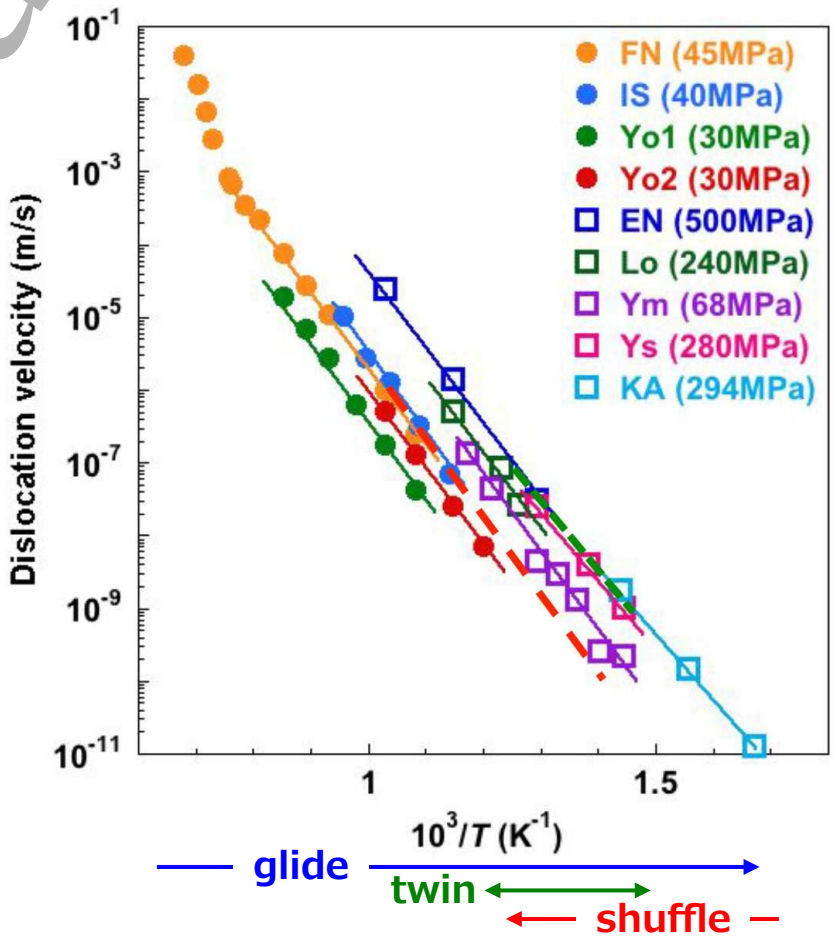

Fig. 2

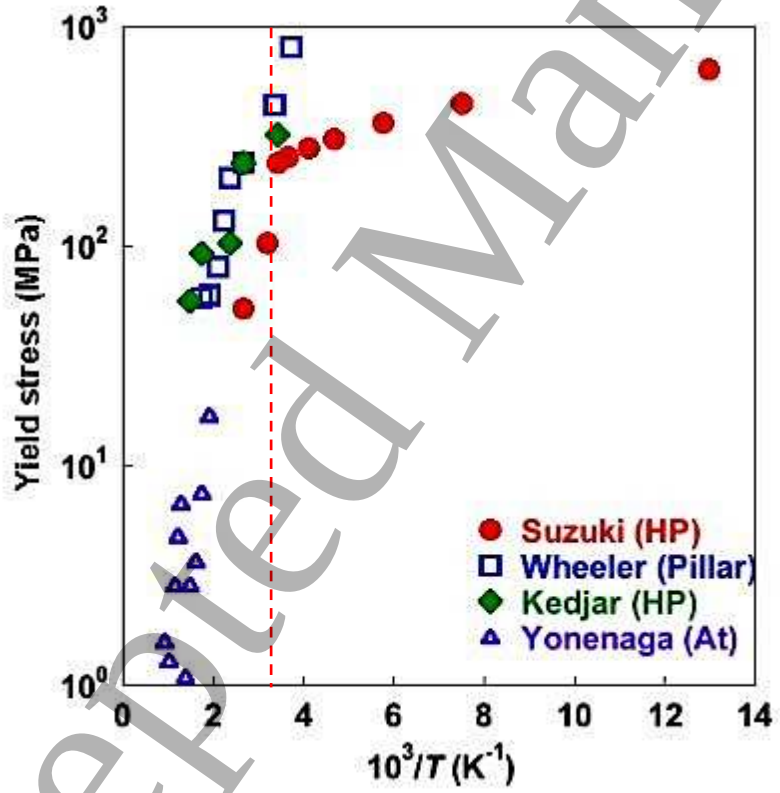

(*a*)

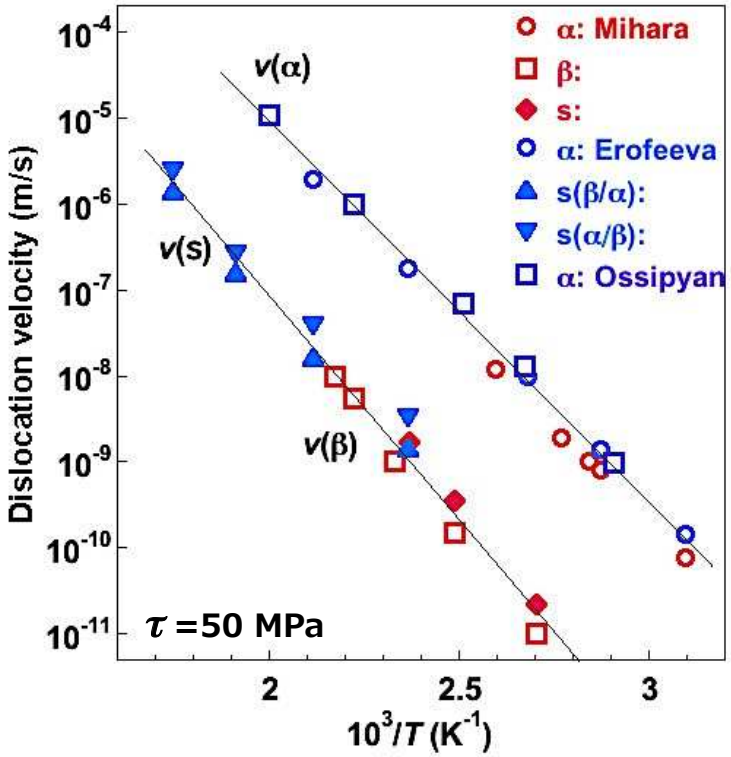

(*b*)

Fig. 3

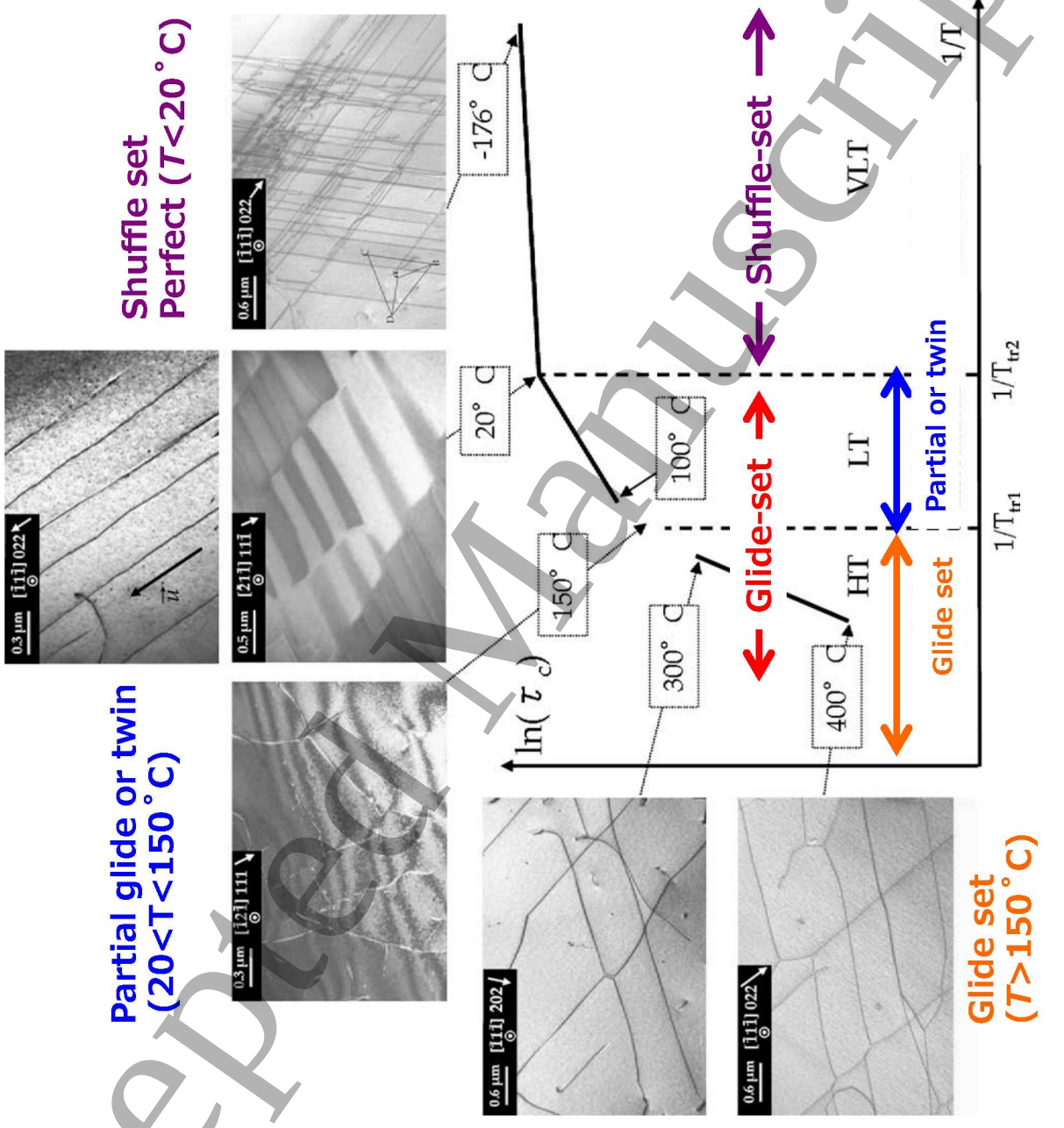

Fig. 4

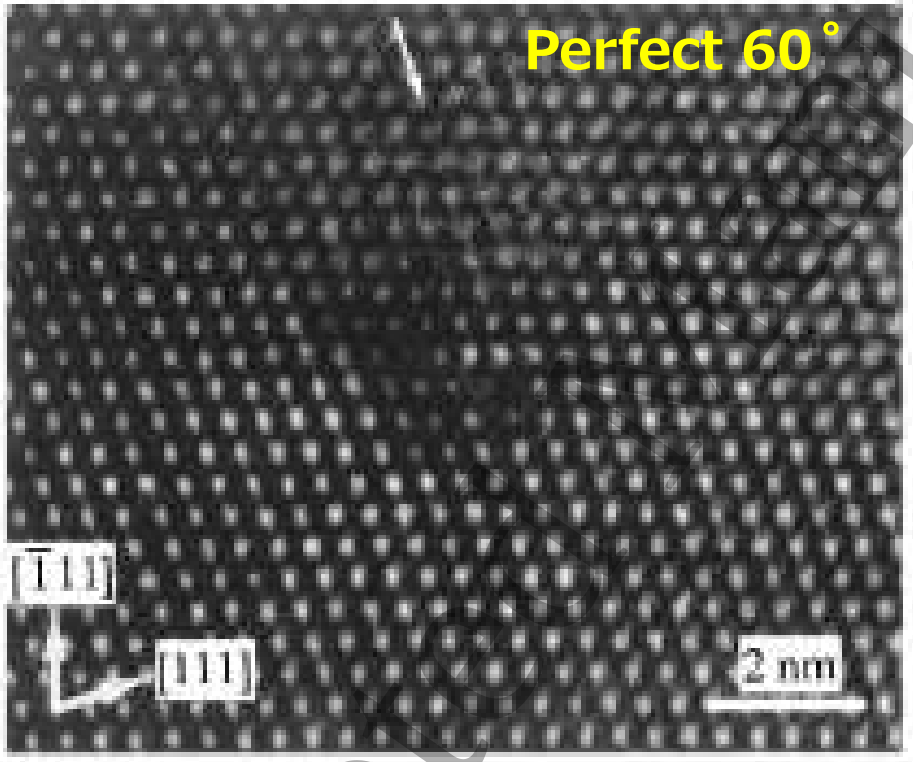

(*a*)

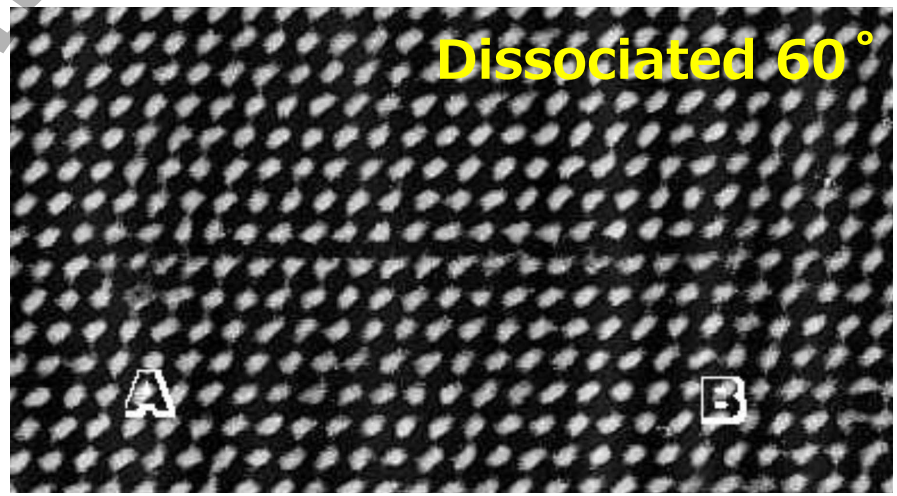

(*b*)

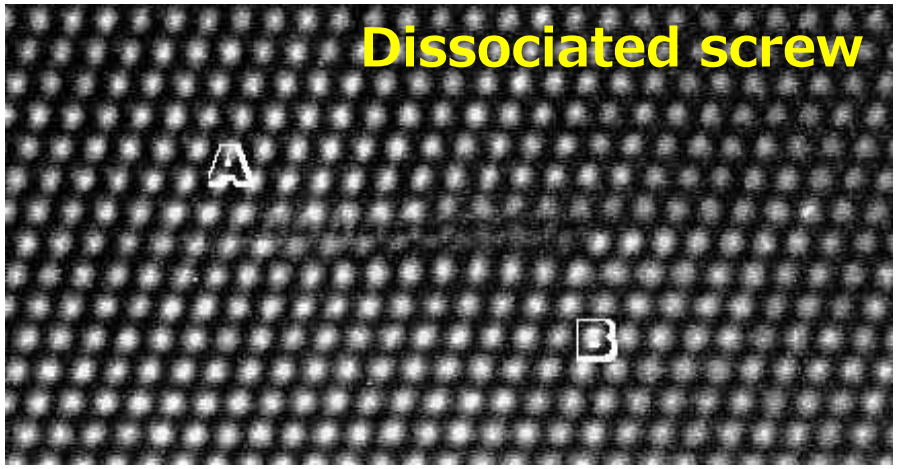

(*c*)

Fig. 5

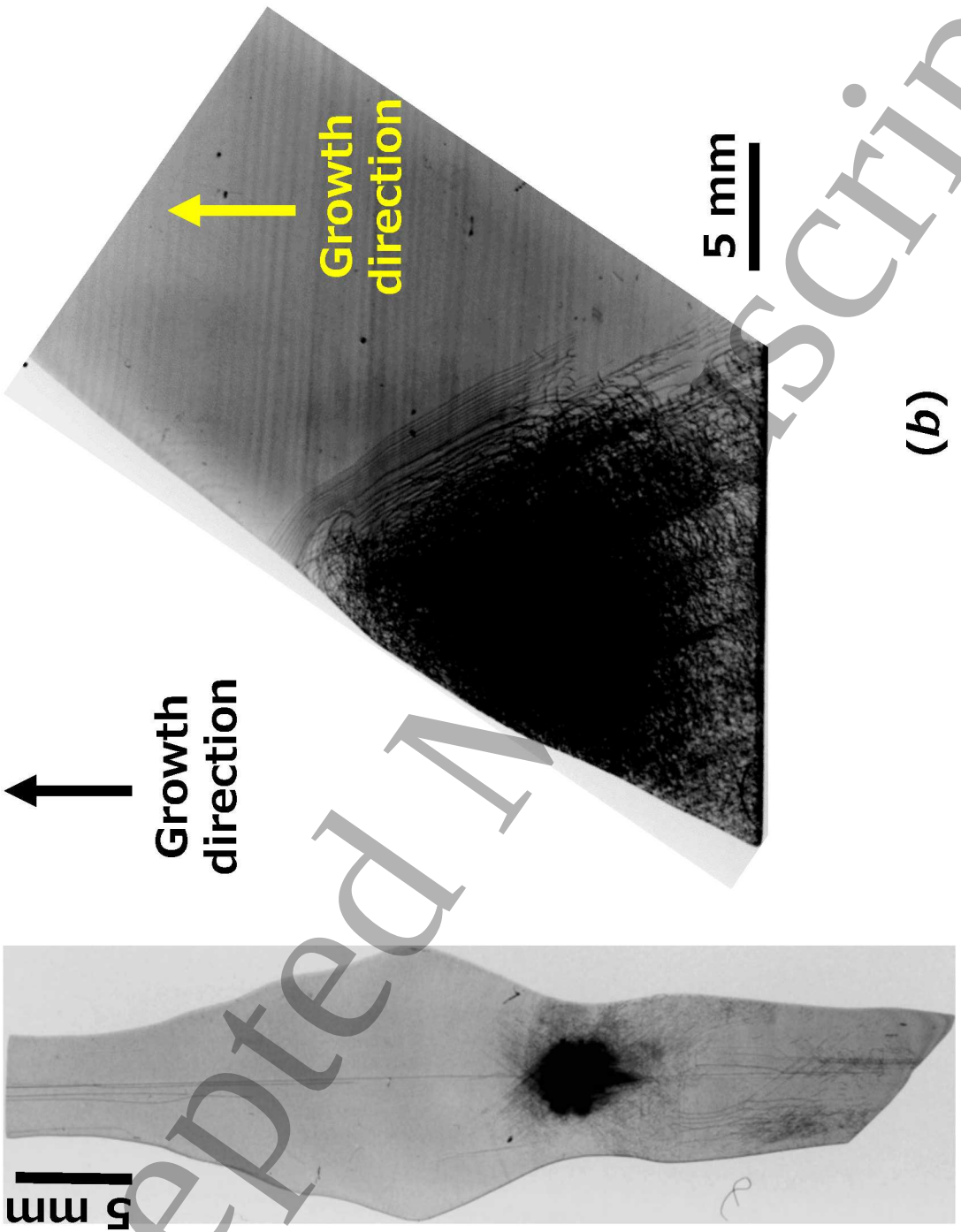

Fig. 6

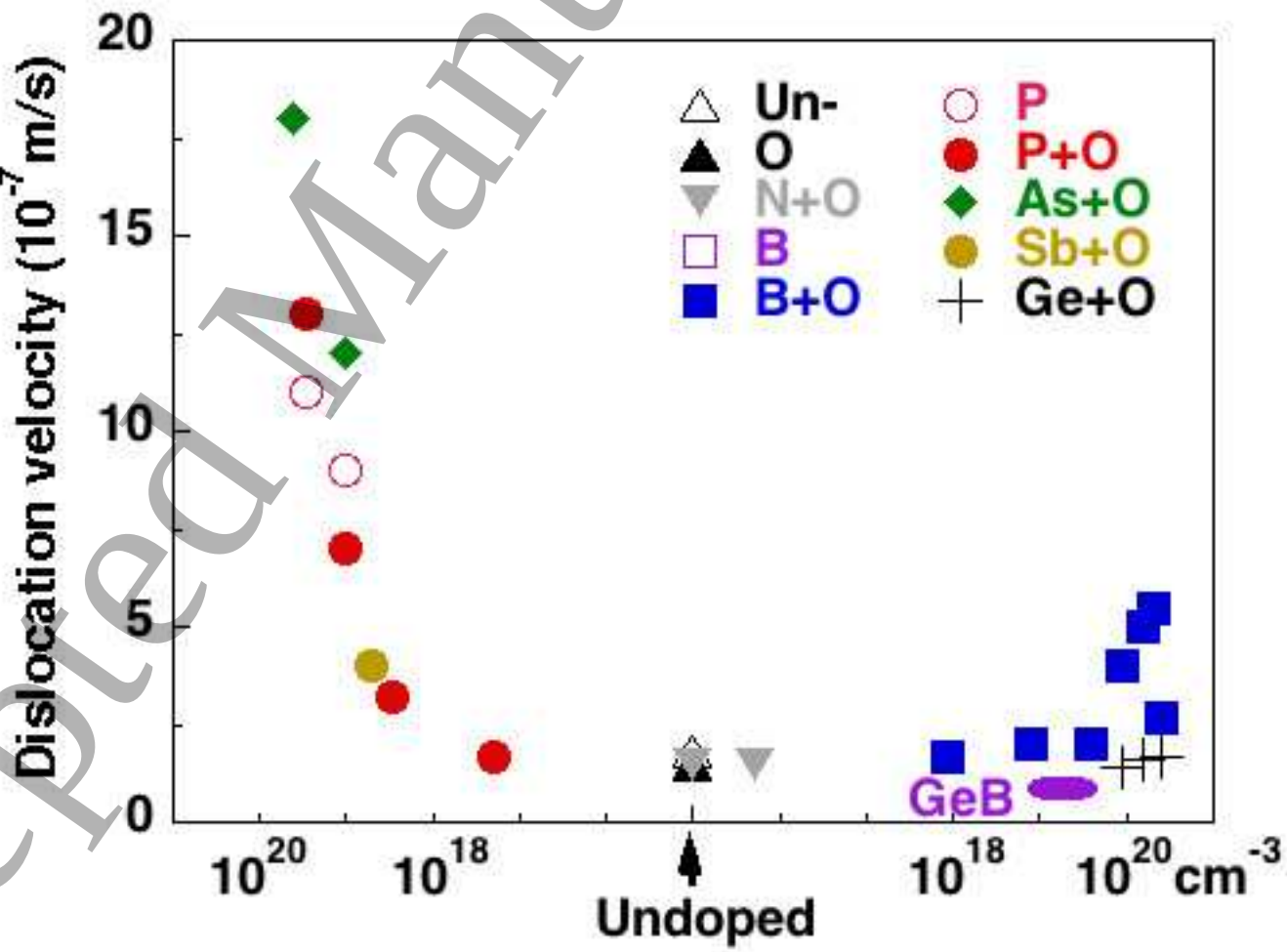

Fig. 7

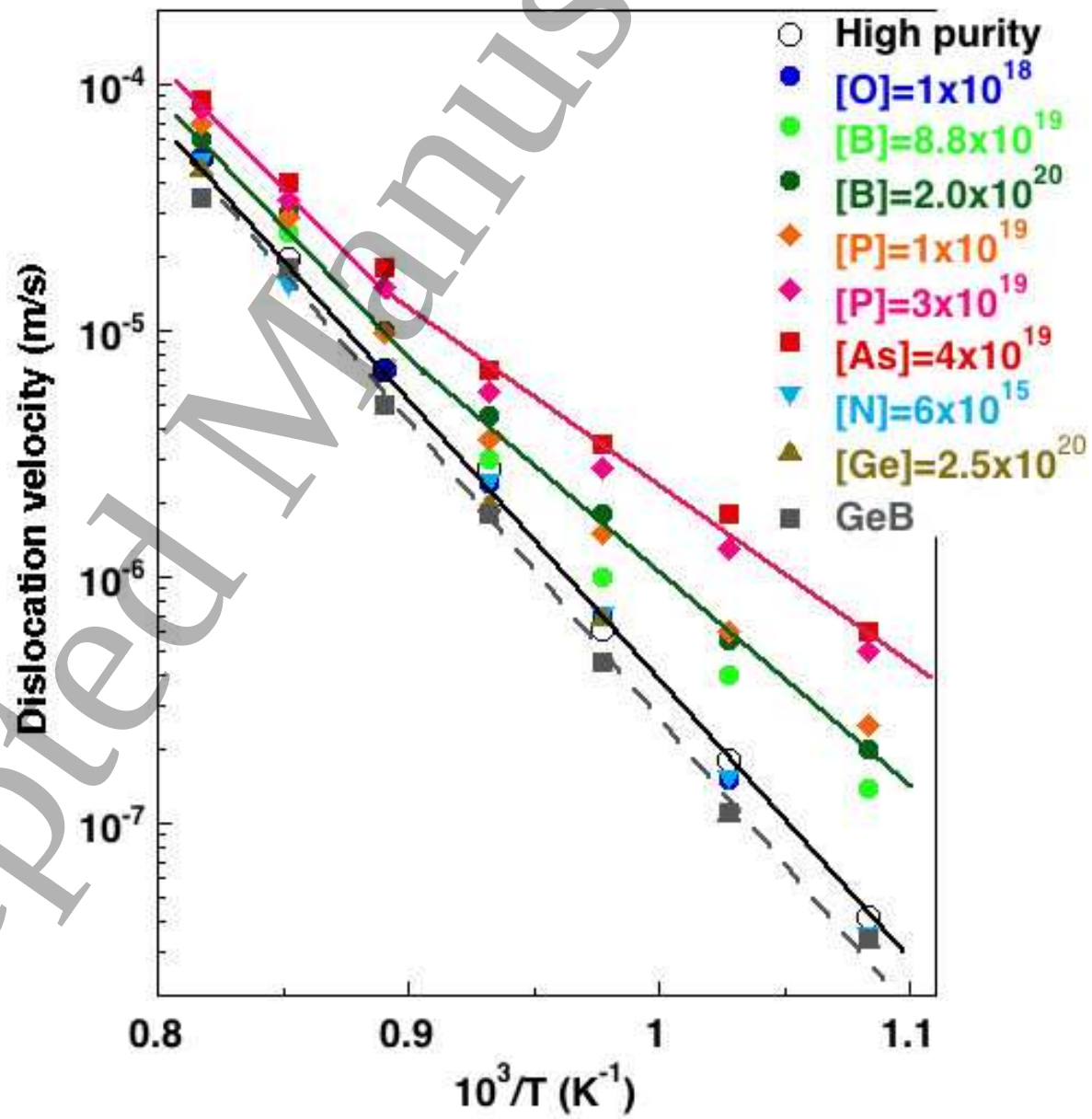

Fig. 8

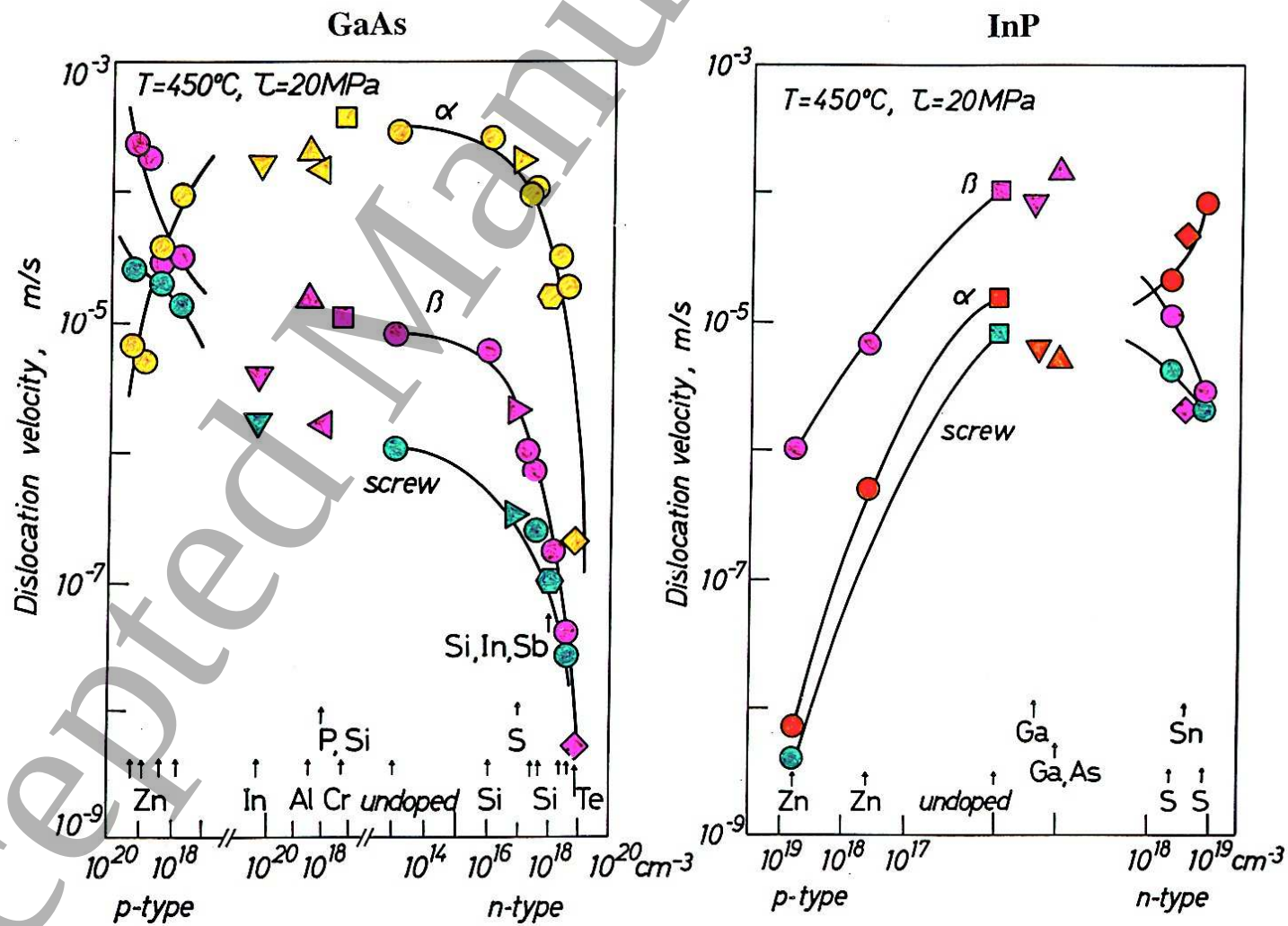

Fig. 9

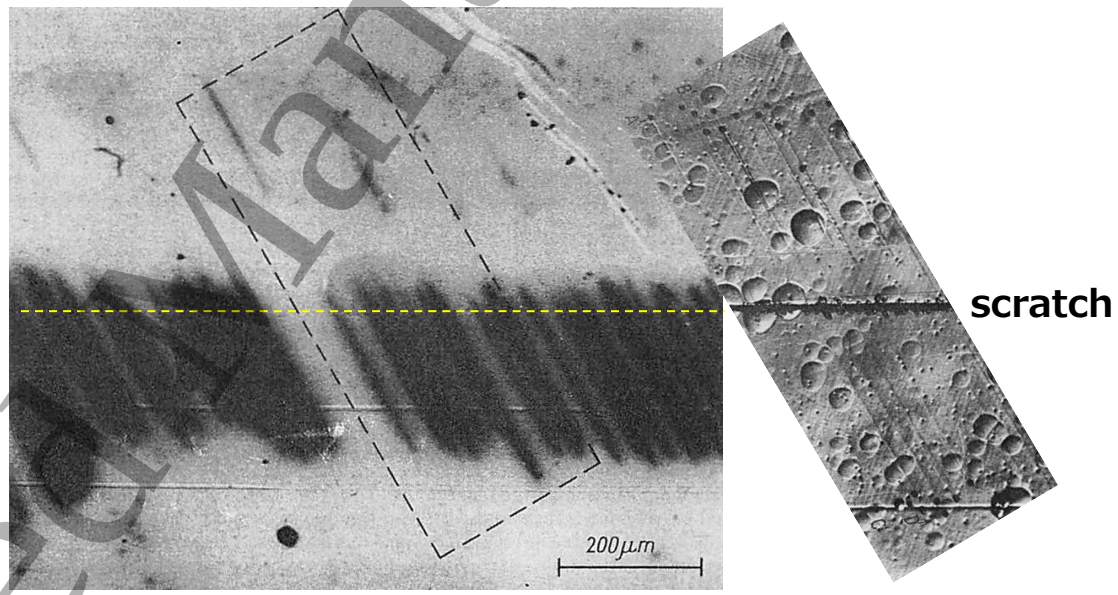

Fig. 10

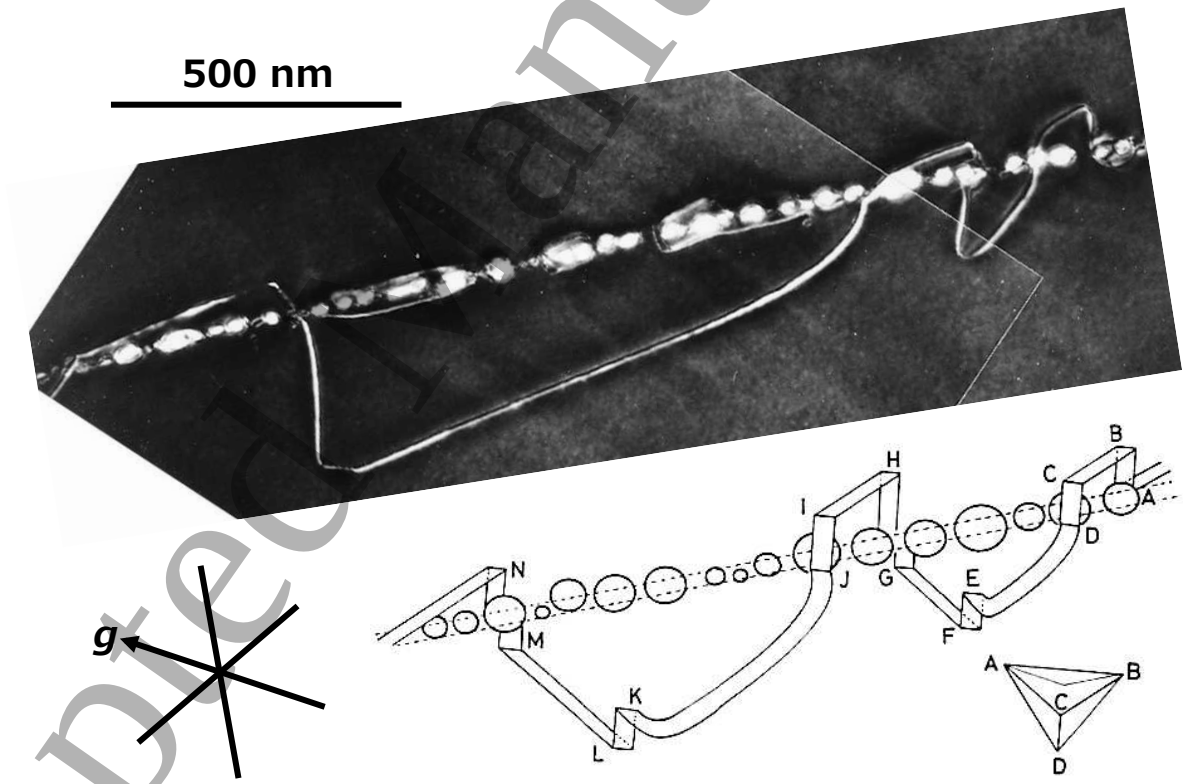

Fig. 11

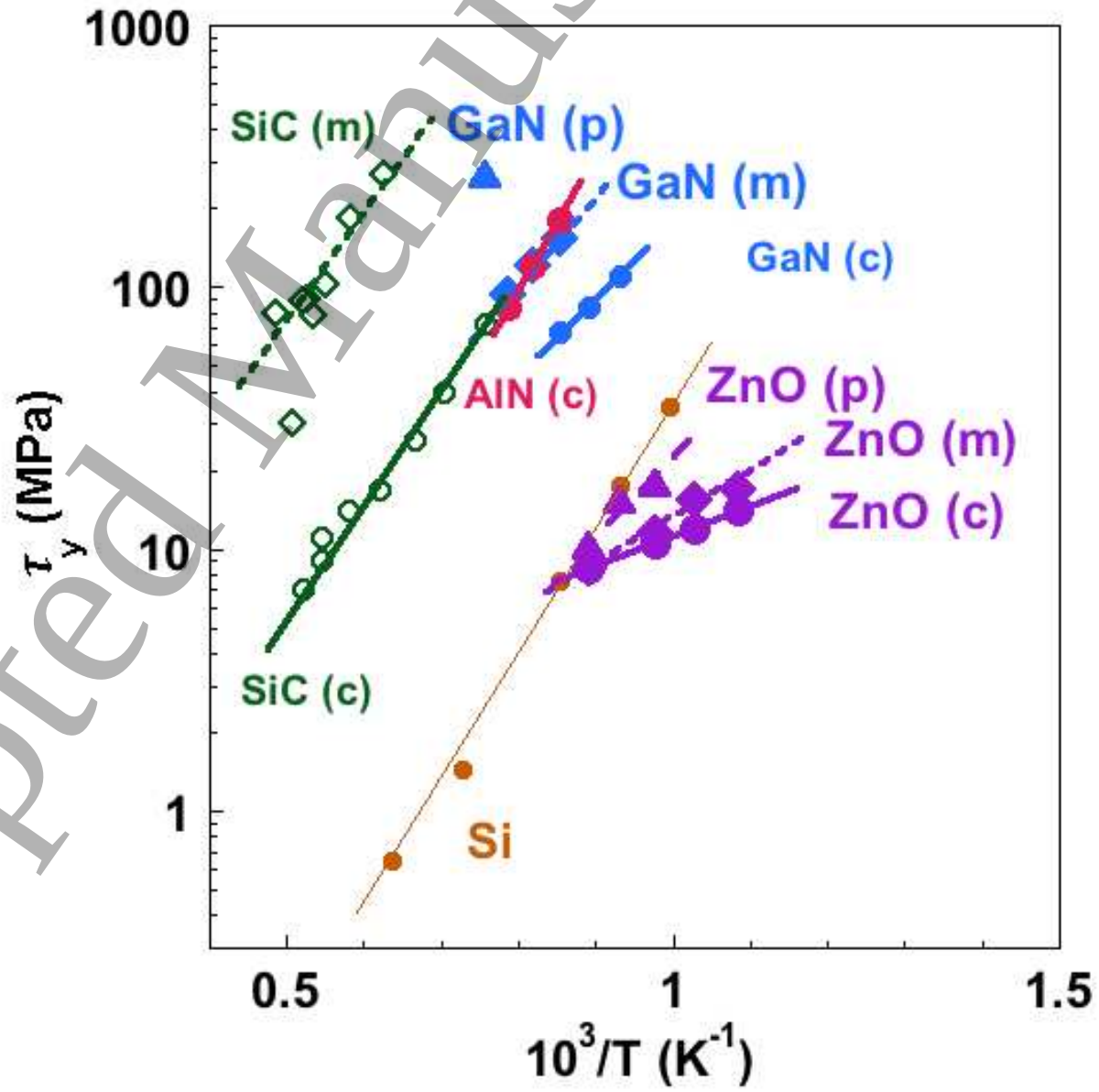

Fig. 12

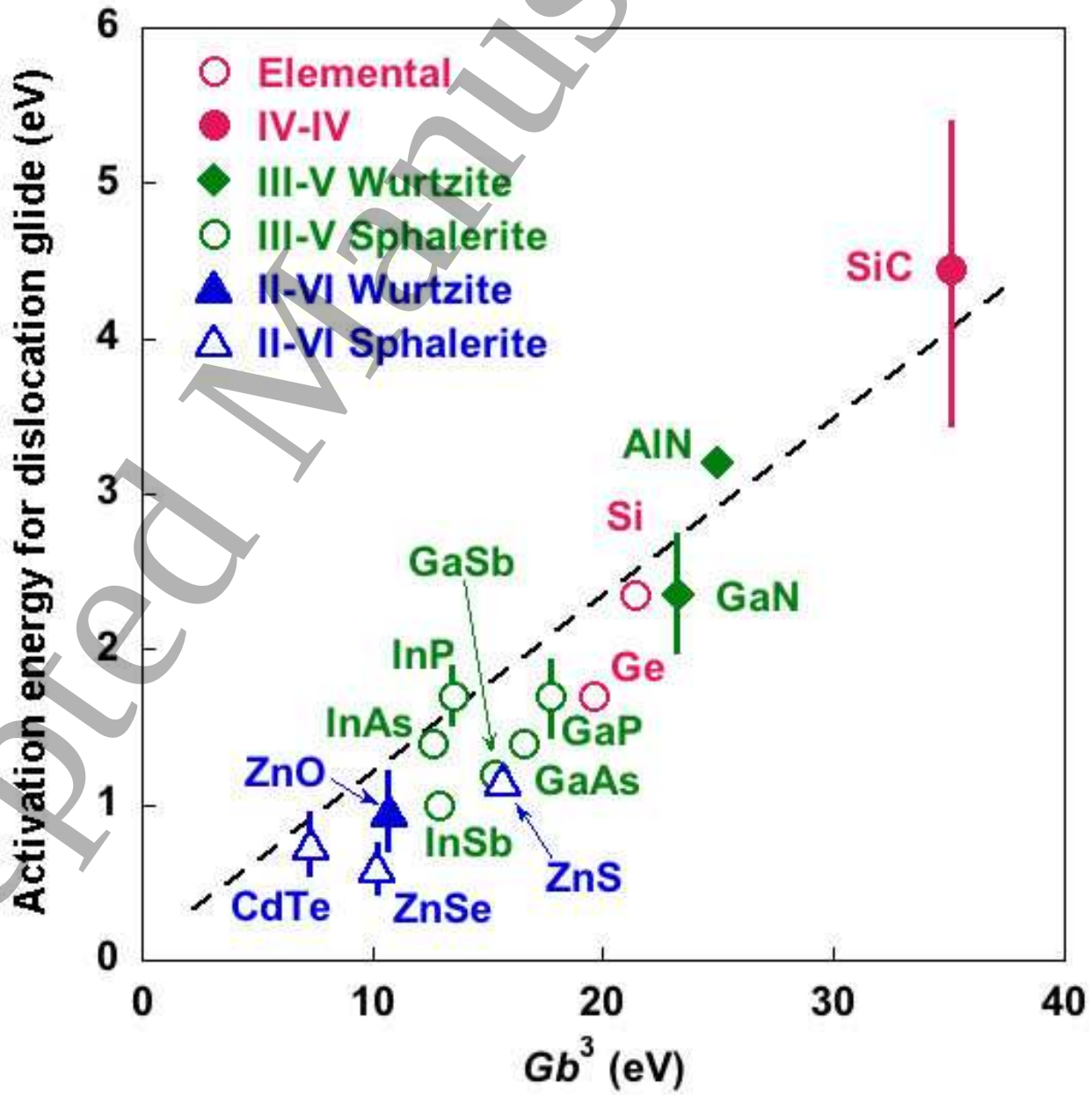

Fig. 13